REGULAR PAPER

Design, Analysis and Simulation of RF MEMS Capacitive Shunt Switch with Perforations for Ka-Band Applications

K. Srinivasa Rao[1] · K. Girija Sravani[1,2] · Y. Akhil Chowdary[1] · P. Naveena[1] · K. Vedha Vyasa[1] · Himanshu Raina[1] · B. Deepa Sunanda[1]

Abstract

This paper presents the design and analysis of an RF MEMS Shunt switch with low pull-in voltage and good RF performance. The switch includes a vertically deforming beam which includes perforations and meanders. This switch is developed to run at a Radio Frequency (RF) of 35 GHz. The significant accomplishments in this work are the pull in voltage that is minimized to 3.72 V, and the return loss is listed below −26.6 dB, the insertion loss is listed less than −0.22 dB and isolation is −36.4 dB. The up and down capacitance of the switch is 110 fF, 1.58 pF, and the obtained capacitance ratio is 113.5. The product utilized for the CPW line is Gold (Au). The dielectric product utilized in between the beam and the CPW transmission line is Silicon Nitride (Si_3N_4). We achieved electromechanical analysis through COMSOL software and RF analysis is done using HFSS software.

1 Introduction

The RF MEMS have been shown as one of the most important innovations in the design of modern pioneering communication applications, due to their low power usage, less insertion loss, and excessive isolation, and high linearity. MEMS switches have an exceptional RF efficiency contrasted with p-i-n diodes and field-effect transistors (FET) [1–3]. MEMS switches are classified as shunt and series capacitive switches depending upon their electrical setup. The switch created in this document is a shunt fixed-fixed switch that is effective at 35 GHz and can be utilized in ka band applications such as satellite and military applications and automobile speed detection. The restriction of the RF MEMS switch is its lifetime reliability. It can't endure temperature level modifications and humidity effects [4]. It can't hold up against to vibration and shocks. The polysilicon product utilized in the building procedure is a Brittle material.

RF MEMS shunt switches with serpentine spring structures have been utilized to accomplish low actuation voltage keeping adequate low isolation [5]. RF MEMS switches could not certify business requirements since of their bad reliability [6]. Several procedures have been conveyed. Amid these dielectric charging has been a significant issue. Issues based upon self-actuation because of excessive RF power and switches that do not self-actuate have been demonstrated [7]. Low loss fixed-fixed RF MEMS capacitive switches at greater frequencies and modeling of devices for design and optimization and gadget reliability [8]. Research studies and simulations mention that rectangle-shaped perforations offer much better outcomes compared to round and square type perforations [9]. A comparable switch is examined over a frequency variety of 0.6–40 GHz. they have accomplished an actuation voltage of 4.2 V at 0.9 μm and the insertion and return losses are −0.44 and −16 dB by utilizing dielectric material as aluminium nitride (AlN) and the material utilized for the beam is gold.

In this paper, an RF MEMS fixed-fixed switch is designed and simulate as spring constant, pull-in voltage

✉ K. Srinivasa Rao
drksrao@kluniversity.in

1   Department of ECE, MEMS Research Group, Koneru Lakshmaiah Educational Foundation (Deemed to be University), Green Fields, Vaddeswaram, Guntur 522502, India

2   Department of Electronics and Communication Engineering, MEMS Design Center, National Institute of Technology, Silchar, Assam 788010, India
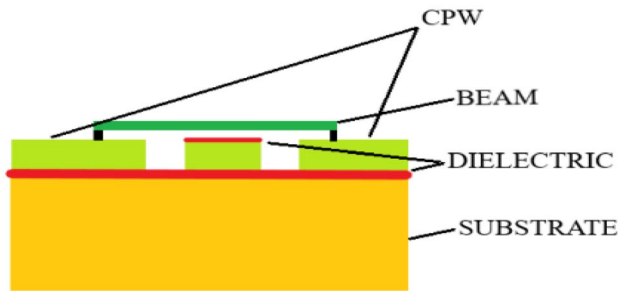
Fig. 1 Schematic of RF MEMS Shunt switch

Fig. 2 Top view of proposed RF MEMS switch

switching time, and quality factor are computed. We validate the outcomes utilizing COMSOL software application and HFSS software application. The insertion losses and isolation losses are determined utilizing the HFSS software application. The graphs between voltage and displacement, switching time, losses, and the downstate capacitance and upstate capacitance are calculated.

The paper is arranged as follows, in Sect. 2 the design of the planned RF MEMS switch is debated, and the materials utilized in the building and construction of the switch are discussed. In Sect. 3 numerous outcomes such as pull-in voltage, spring constant, switching time, and Cd and Cu ratio examination of the switch and the RF performance features such as insertion and return losses in ON state and isolation losses in OFF state have been discussed. Section 4 concludes the entire paper.

Fig. 3 Switch Simulation at pull—in voltage 3.72 V

2 Proposed Device and Its Specifications

The proposed RF MEMS switch is a shunt fixed-fixed switch. Through optimization, we acquire the height of substrate as 650 μm or below it, and above the substrate, the CPW layer is formed. The CPW space and the width of the signal line is selected to attain a specific impedance of 50 Ω. The space in between CPW lines is 45/75/45 is attained through conformal mapping which is nothing but a coordinate transformation technique and can be suitable for planar and non-planar transmission lines. The beam is of thickness 2 μm is holding at a height of 3 μm overhead the CPW line. The beam is integrated with square holes of 8 μm and meanders are placed at the same height as the beam and the layer of the switch is placed above the signal line utilizing anchors which are placed at the corner of each meander. The meanders are of the same thickness as the switch and positioned at the same height (Figs. 1, 2, 3, 4, 5, 6).

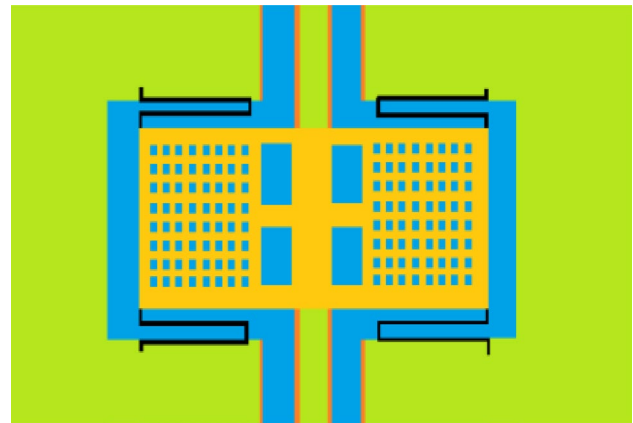The proposed switch dimensions are given in Table 1.

Fig. 4 Voltage vs displacement

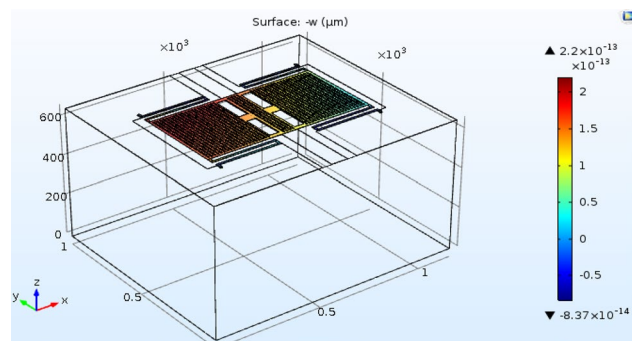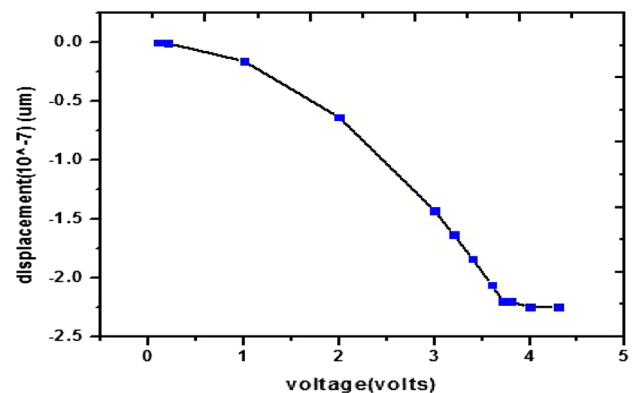## 3 Results and Discussions

3.1 Pull-in Voltage

The pull-in voltage of the proposed switch is associated with the membrane attached to the fixed–fixed beam and
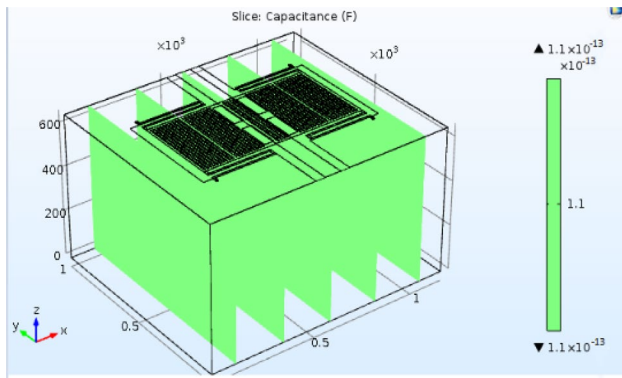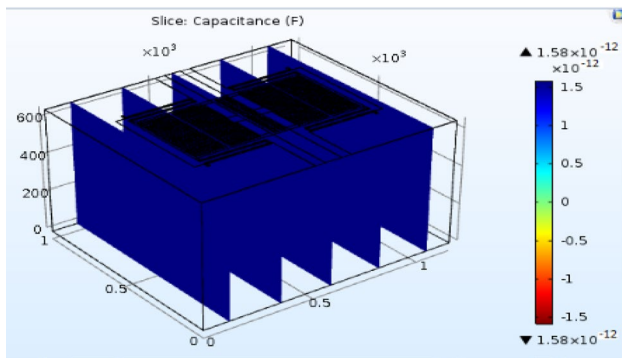
Fig. 5 Up state capacitance of the switch

Fig. 6 Down state capacitance of the switch

Table 1 Specifications of the proposed design

S. no	Component	Length (µm)	Width (µm)	Depth (µm)	Material
1	Substrate	1165	1000	650	Silicon
2	CPW (G/S/G)	75	1000	1.2	Gold
3	Beam	784	392	2	Gold
4	Perforations	8	8	2	–
9	Dielectric layer	75	1000	0.2	Si_3N_4

Ohmic contact can be obtained from Eq. (1) [10],

$$V_p = \sqrt{\frac{8kg_0^3}{27\varepsilon_0 A}} \tag{1}$$

where 'K' is the obtained spring constant, 'ε_0' $= 8.85 \times 10^{-12}$ F/m is the free space permittivity and 'A' is the covering area of CPW and beam.

The pull in voltage mainly depends on the spring constant (K), the gap between CPW and beam, A is the overlapping area. As spring constant increases pull-in voltage increases. Reducing the value of 'K' is the best way to reduce the pull in voltage. Pull in voltage can also be decreased by Increasing the Area. The spring constant or spring stiffness of the beam is obtained by [11],

$$K = \frac{Ewt^3}{4l^3} \tag{2}$$

where 'w' is the width of the beam, 'l' are the length of the beam, 't' is the thickness, 'E' is the young's modulus. From the Eq. (2) the spring stiffness of the beam is obtained as 0.44989 N/m.

Thus, the pull-in voltage of the switch is attained by replacing the value of k and the value of the 'g_0' in Eq. (1) and it is obtained theoretically as 3.72 V.

The behavioral features of the switch are simulated by using the COMSOL 5.2 tool. Potential difference is applied across the lower and upper actuation electrodes which cause the actuation of the switch.

3.2 Capacitance Analysis

Variation of capacitance with voltage applied between electrodes is plotted by electrostatic analysis. Good dielectric materials generally have a relative permittivity between 3.4 and 13. In the switch discussed, a dielectric material is taken as silicon nitride which has a dielectric constant of 9.5. The up capacitance of the switch can be assessed by the equation [12].

$$C_u = \frac{\varepsilon_0 A}{g + \frac{t_d}{\varepsilon_r}} \tag{3}$$

The down state capacitance is given by

$$C_d = \frac{\varepsilon_0 \varepsilon_r A}{t_d} \tag{4}$$

where 'ε_0' is the free space permittivity, 'ε_r' dielectric layer permittivity, 'A' is the overlapping area, g is the gap between the electrodes and t_d is the thickness of dielectric layer.

The up and down state capacitance are calculated methodically from the above equations are 110 fF and 1.58 pF. The capacitance ratio of 113.50 is attained from the switch proposed.

3.3 Resonance Frequency

The maximum displacement of the switch takes place at the resonant frequency. The space among the electrodes in

the switch is taken as 3 μm. The frequency of the switch is obtained by the equation [13].

$$F_r = \frac{1}{2\pi}\sqrt{\frac{K}{m}} \tag{5}$$

where 'm' is the effective mass of the beam and 'K' is the spring constant of the beam. The resonant frequency is calculated as 7.1 kHz.

3.4 Quality Factor

The quality factor is the function of spring constant, resonant frequency and the damping coefficient. The structure of the membrane defines the damping coefficient and there are many methods for reducing the damping ratio. The damping coefficient is obtained from the equation,

$$b = \frac{3}{2\pi}\frac{\mu A^2}{g^3} \tag{6}$$

where 'μ' $= 1.885 \times 10^{-5}$ is air viscosity, g is the gap and 'A' is the overlapping area. Thus, the quality factor is obtained from,

$$Q = \frac{K}{2\pi f_0 b} \tag{7}$$

The damping ratio and quality factor are 2.8×10^{-4} and the quality factor is 7.1×10^{-9}.

3.5 Switching Time Analysis

The applied voltage is responsible for the changes in the switching time. Greater the applied voltage stronger the electrostatic forces acting on the beam to displace it. Switching speed defines the device performance. The switching time is given by the equation [14–17]

$$T_s = \frac{3.67 V_p}{V_s \omega_0} \tag{8}$$

where V_s is the actuation voltage and the pull-in voltage is Vp, ($V_s = 1.4 V_p$) and ω_0 is the angular resonant frequency.

The switching period of the proposed switch is calculated by using the above equation and a graph is drawn for different voltages as shown in Fig. 7.

3.6 RF-Performance Analysis

The RF performance is analyzed in the ON and OFF state of the switch. The return and insertion are measured in the ON state, and the isolation is in the OFF state. By reducing the number of connectors or selecting low insertion loss devices we can achieve low insertion loss. As power is expensive at greater frequencies, electromechanical switches provide the lowest possible loss along the transmission line [18–20]. The S-parameters of return, insertion, and isolations are shown in Figs. 8, 9, and 10.

The return and insertion losses are obtained as -26.6, -0.22 dB at 31 GHz, and the isolation measured as -36.4 dB at 35 GHz frequency.

4 Conclusion

This work displays the design and simulation of a capacitive shunt RF MEMS fixed–fixed switch analyzed at a frequency of 35 GHz. The actuation structure used in this paper is

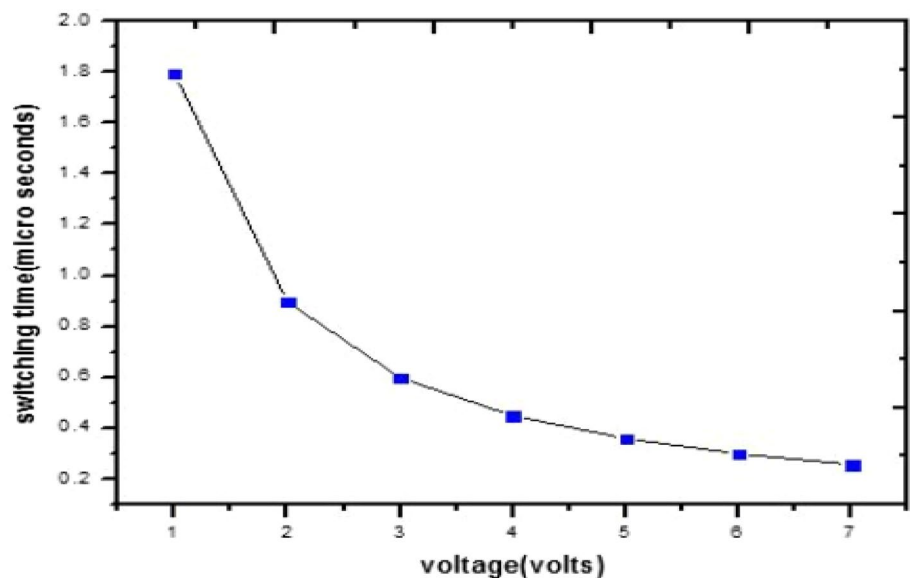**Fig. 7** Switching time graph of the switch

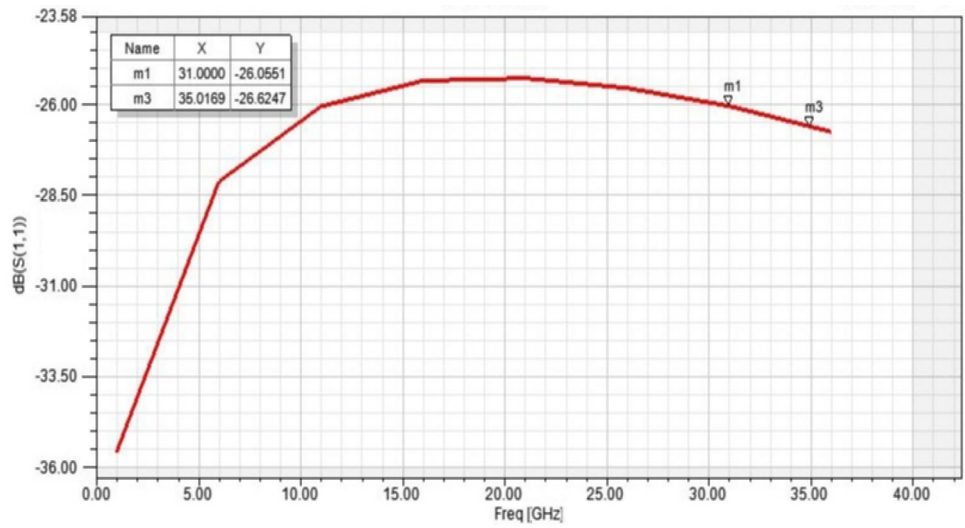**Fig. 8** Measured Return loss (S_{11}) at 31 GHz

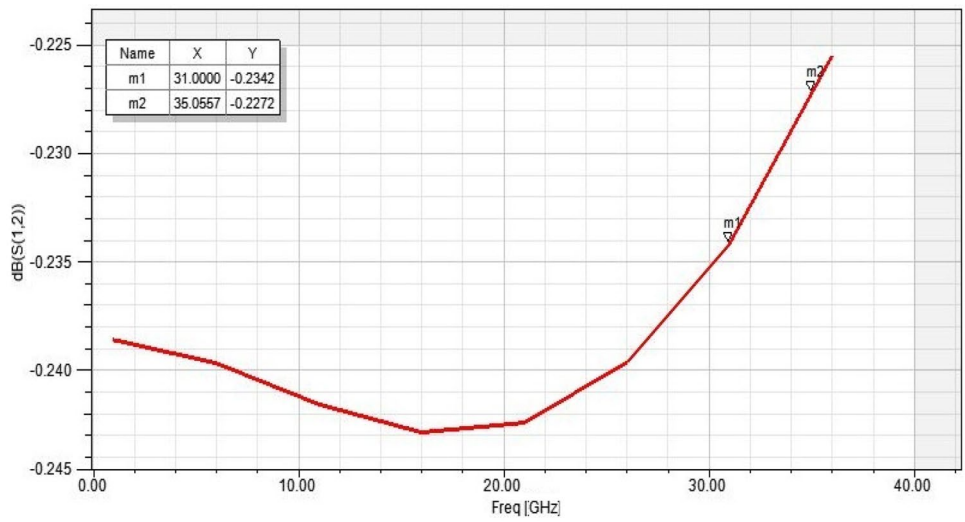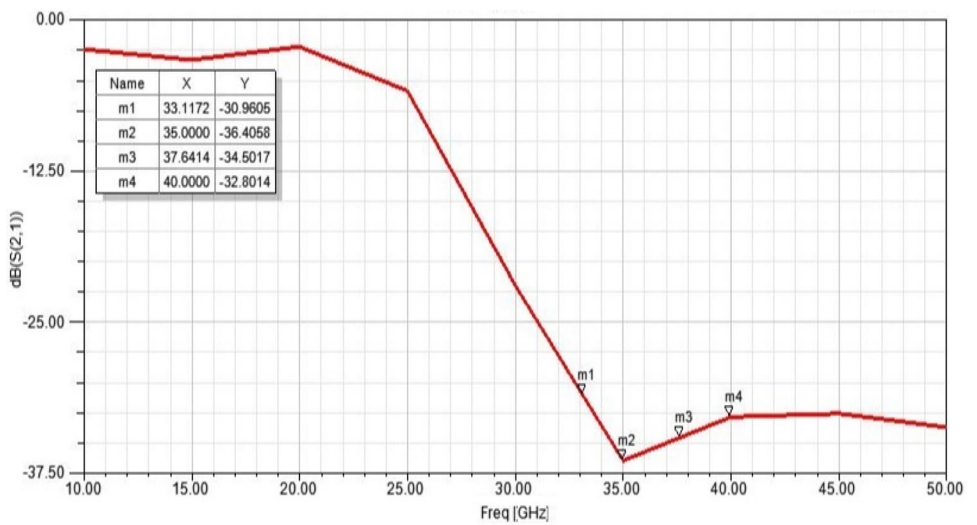**Fig.9** Insertion (S_{12}) of the switch at 31 GHz

Fig. 10 Isolation of proposed switch at 35 GHz

anchored with the help of meanders having holes on the membrane which helps to reduce the pull-in voltage of the switch. By implementing the electromechanical analysis, the spring constant of the switch is observed as 0.44 N/m and a pull-in voltage of 3.72 V is obtained from the simulations. The switch is simulated in HFSS software. It exhibits insertion and return loss of -0.22 and -26.6 dB, and the isolation of -36.4 dB at 35 GHz. Based on the performance of the switch it can be used for Ka-band Radar applications.

References

1. R.E. Mihailovich, M. Kim, J.B. Hacker, E.A. Sovero, J. Studer, J.A. Higgins, MEM relay for reconfigurable RF circuits. IEEE Microw. Wirel. Compon. Lett. **11**(2), 53–55 (2001)

2. Hyman D, Lam J, Warneke B, Schmitz A, Hsu TY, Brown J, Schaffner J et al (1999) Surface-micromachined RF MEMs switches on GaAs substrates. Int. J. RF Microw. Computer-Aided Eng. Co-sponsored Center Adv. Manuf. Packag. Microw. Opt. Dig. Electron (CAMPmode) Univ. Colorado Boulder 9(4): 348–361

3. P.M. Zavracky, N.E. McGruer, R.H. Morrison, D. Potter (1999) Microswitches and microrelays with a view toward microwave applications. Int. J. RF Microw. Computer-Aided Eng. Co-sponsored Center Adv. Manuf. Packag. Microw. Opt. Dig. Electron (CAMPmode) Univ. Colorado Boulder 9(4): 338–347

4. Y. Zhu, H.D. Espinosa, Effect of temperature on capacitive RF MEMS switch performance—a coupled-field analysis. J. Micromech. Microeng. **14**(8), 1270 (2004)

5. S.P. Pacheco, L.P. Katehi, C.C. Nguyen (2000) Design of low actuation voltage RF MEMS switch, in 2000 IEEE MTT-S international microwave symposium digest (Cat. No. 00CH37017), vol. 1. IEEE, pp. 165–168

6. E.R. Brown, RF-MEMS switches for reconfigurable integrated circuits. IEEE Trans. Microw. Theory Tech. **46**(11), 1868–1880 (1998)

7. D. Peroulis, S.P. Pacheco, L.P. Katehi, RF MEMS switches with enhanced power-handling capabilities. IEEE Trans. Microw. Theory Tech. **52**(1), 59–68 (2004)

8. S.K. Thakur, K.A. SumithraDevi, I. Ranjitha (2009) Performance of low loss RF MEMS fixed-fixed capacitive switch characterization, in 2009 applied electromagnetics conference (AEMC). IEEE, pp. 1–4

9. A.K. Ravirala, L.K. Bethapudi, J. Kommareddy, B.S. Thommandru, S. Jasti, P.R. Gorantla, A. Puli, G.S. Karumuri, S.R. Karumuri, Design and performance analysis of uniform meander structured RF MEMS capacitive shunt switch along with perforations. Microsyst. Technolo. **24**(2), 901–908 (2018)

10. M. Angira, K. Rangra, Design and investigation of a low insertion loss, broadband, enhanced self and hold down power RF-MEMS switch. Microsyst. Technol. **21**(6), 1173–1178 (2015)

11. H.R. Ansari, S. Khosroabadi, "Design and simulation of a novel RF MEMS shunt capacitive switch with a unique spring for Ka-band application. Microsyst. Technol. **25**(2), 531–540 (2019)

12. T. Lakshmi Narayana, K. Girija Sravani, K. Srinivasa Rao, Design and analysis of CPW based shunt capacitive RF MEMS switch. Cogent Eng. **4**(1), 1363356 (2017)

13. A. Chakraborty, B. Gupta, B.K. Sarkar, Design, fabrication and characterization of miniature RF MEMS switched capacitor based phase shifter. Microelectron. J. **45**(8), 1093–1102 (2014)

14. T. Lakshmi Narayana, K. Girija Sravani, K.A. Srinivasa Rao, A micro level electrostatically actuated cantilever and metal contact based series RF MEMS switch for multi-band applications. Cogent Eng. **4**(1), 1323367 (2017)

15. X.J. He, B.S. Jin, Q. Wu, J.H. Yin (2006) Time response and dynamic behavior of electrostatic driven RF MEMS capacitive switches for Phase Shifter Applications. in 2006 IEEE antennas and propagation society international symposium. IEEE, pp. 1965–1968

16. K.G. Sravani, K. Guha, K.S. Rao, Analysis on selection of beam material for novel step structured RF-MEMS switch used for satellite communication applications. Trans. Electr. Electr. Mater. **19**(6), 467–474 (2018)

17. K.G. Sravani, K.S. Rao, Analysis of RF MEMS shunt capacitive switch with uniform and non-uniform meanders. Microsyst. Technol. **24**(2), 1309–1315 (2018)

18. K.S. Rao, C.G. Chand, K.G. Sravani, D. Prathyusha, P. Naveena, G.S. Lakshmi, P.A. Kumar, T.L. Narayana, Design, modeling and analysis of perforated RF MEMS capacitive shunt switch. IEEE Access **7**, 74869–74878 (2019)

19. K.G. Sravani, D. Prathyusha, K.S. Rao, P.A. Kumar, G.S. Lakshmi, C.G. Chand, P. Naveena, L.N. Thalluri, K. Guha, Design and performance analysis of low pull-in voltage of dimple type capacitive RF MEMS shunt switch for Ka-band. IEEE Access **7**, 44471–44488 (2019)

20. K.G. Sravani, D. Prathyusha, G.R. Prasad, C.G. Chand, P.A. Kumar, K. Guha, K.S. Rao, Design of reconfigurable antenna by capacitive type RF MEMS switch for 5G applications. Microsyst. Technol. **7**, 1–9 (2020)